

Rotator Cuff Repair and Overlay Augmentation by Direct Interlocking of a Nonwoven Polyethylene Terephthalate Patch Into the Tendon

Evaluation in an Ovine Model

Dominik C. Meyer,* MD, Elias Bachmann,*^{†‡} MSc, Salim Darwiche,^{§||} PhD, Andrea Moehl,[‡] MSc, Brigitte von Rechenberg,^{§||} DVM ECVS, Christian Gerber,* MD, and Jess G. Snedeker,*^{†¶} PhD
Investigation performed at University of Zurich, Zurich, Switzerland

Background: Arthroscopic repair of large rotator cuff tendon tears is associated with high rates of retear. Construct failure often occurs at the suture-tendon interface. Patch augmentation can improve mechanical strength and healing at this interface.

Purpose: To introduce a novel technique for suture-free attachment of an overlaid patch and evaluate its biomechanical strength and biological performance.

Study Design: Descriptive and controlled laboratory studies.

Methods: An established ovine model of partial infraspinatus tendon resection and immediate repair was used. After a nonwoven polyethylene terephthalate patch was overlaid to the resected tendon, a barbed microblade was used to draw fibers of the patch directly into the underlying tissue. In vivo histological assessment of healing was performed at 6 and 13 weeks after implantation. Ex vivo models were used to characterize primary repair strength of the suture-free patch fixation to tendon. Additional ex vivo testing assessed the potential of the technique for patch overlay augmentation of suture-based repair.

Results: The in vivo study revealed no macroscopic evidence of adverse tissue reactions to the interlocked patch fibers. Histological testing indicated a normal host healing response with minimal fibrosis. Uniform and aligned tissue ingrowth to the core of the patch was observed from both the tendon and the bone interfaces to the patch. There was no evident retraction of the infraspinatus muscle, lengthening of the tendon, or tendon gap formation over 13 weeks. Ex vivo testing revealed that direct patch interlocking yielded tendon purchase equivalent to a Mason-Allen suture (150 ± 58 vs 154 ± 49 N, respectively; $P = .25$). In an overlay configuration, fiber interlocked patch augmentation increased Mason-Allen suture retention strength by 88% (from 221 ± 43 N to 417 ± 86 N; $P < .01$) with no detectable difference in repair stiffness.

Conclusion: Testing in an ovine model of rotator cuff tendon repair suggested that surgical interlocking of a nonwoven medical textile can provide effective biomechanical performance, support functional tissue ingrowth, and help avoid musculotendinous retraction after surgical tendon repair.

Clinical Relevance: The novel technique may facilitate patch augmentation of rotator cuff repairs.

Keywords: rotator cuff repair; patch augmentation; biomaterials; in vivo; sheep model; biomechanics

Rotator cuff tears present a major socioeconomic burden that is exacerbated by high rates of retear after repair surgery.^{4,7,13,32,38} The reasons for unsatisfactory postsurgical healing are multifaceted, with biomechanical, biological, and technical obstacles to success. Mechanical weakness at the suture-tendon interface is widely viewed as

a particularly critical factor, and patch augmentation of this interface has emerged as an active area of research and development.¹¹ Although reported outcomes of patch-based rotator cuff augmentation vary,^{14,15,23,25} the approach can yield improved healing outcomes attributable to increased primary repair strength,^{1,8,22,34} improved biological parameters,^{10,35,44} or both.^{6,10,12,14,41} Regardless of the patching approach used, clinical limitations persist with respect to technical feasibility of patch fixation.^{11,43} The learning curve for patch augmentation can be steep, particularly if sutures are used for fixation, and

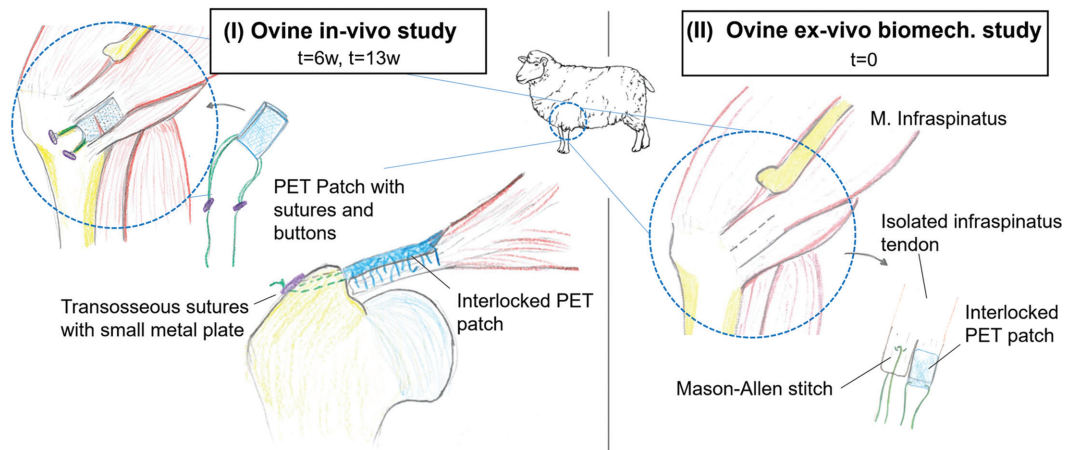


Figure 1. Schematic summary of the 2 study arms using a partially transected ovine infraspinatus tendon model. (Left) An in vivo study was performed using suture-free interlocking of fibers from a nonwoven polyethylene terephthalate (PET) patch into the tendon and reattaching the tendon to its insertional footprint using load-bearing sutures passed only through the patch and not the tendon. (Right) Two ex vivo experimental series were performed, the first assessing the primary strength of a suture-free tendon-to-patch interface as used in the in vivo study and a second assessing the ability of an overlaid patch to mechanically augment an underlying Mason-Allen tendon suture. biomech., biomechanical; t, time; w, weeks.

cumbersome or ineffective patch deployment can meaningfully increase overall costs of the procedure.^{26,28,29,45}

Aiming to overcome some of these limitations, we conceived a suture-free method for surgical attachment of a biomaterial patch to a tendon. This method directly interlocks the fibers of a nonwoven medical felt to an underlying tendon by using a reciprocating barbed blade to draw fibers from the patch directly into the underlying tendon. In this study, we characterize the biomechanical and biological performance of fiber interlocked tendon patches using a sheep model of rotator cuff repair.

METHODS

A 2-part investigation was performed. In the first part, healing was assessed using an in vivo sheep model of rotator cuff repair to characterize biological and histological outcomes of the proposed attachment method. In the second part, primary mechanical performance of the approach was assessed using ex vivo cadaveric models. Both arms of the study were conducted using a partial-transection ovine infraspinatus tendon (Figure 1).

Patch attachment was achieved using a technique based on physical interlocking of nonwoven patch fibers into the underlying tissue by way of a reciprocating microblade. The microblade featured barbs that caught and carried groups of loose fibers within the patch into the tendon (Figure 2). A synthetic polyethylene terephthalate (PET) patch was used for this purpose (SpeedPatch PET R; ZuriMED Technologies AG). PET is a nonabsorbable material that has a long history of use in the orthopaedic field,^{2,3,12,31,33,36,40-42} and its clinical use in nonwoven structures has been investigated in several animal models^{24,30} as well as human application.^{37,39} The surgical device that was used to interlock groups of patch microfibrers into the tendon (FiberLocker Instrument; ZuriMED Technologies AG) runs at a frequency of 42 Hz, with a recommended application time of 17 seconds per square centimeter of patch surface (Figure 3A; Video Supplement 1, available in the online version of this article).

In Vivo Study

In vivo biological response of the interlocked patch implant was characterized using a well-established ovine model of

*Address correspondence to Jess G. Snedeker, PhD, Department of Orthopedics, Balgrist University Hospital, University of Zurich, Forchstrasse 340, CH-8008, Zurich, Switzerland (email: snedeker@ethz.ch).

*Department of Orthopedics, Balgrist University Hospital, University of Zurich, Zurich, Switzerland.

†Institute for Biomechanics, ETH Zurich, Zurich, Switzerland.

‡Musculoskeletal Research Unit, Vetsuisse Faculty, University of Zurich, Zurich, Switzerland.

||Center for Applied Biotechnology and Molecular Medicine (CABMM), University of Zurich, Zurich, Switzerland.

‡ZuriMED Technologies AG, Zurich, Switzerland.

D.C.M. and E.B. contributed equally to this article.

Submitted November 30, 2022; accepted June 5, 2023.

One or more of the authors has declared the following potential conflict of interest or source of funding: J.G.S., E.B., and D.C.M. are coinventors of a patent of the presented technology, jointly filed by the University of Zurich and ZuriMED Technologies. A.M. and E.B. are employed by ZuriMED Technologies. J.G.S., C.G., E.B., and the family of D.C.M. are shareholders in ZuriMED Technologies. AOSM checks author disclosures against the Open Payments Database (OPD). AOSM has not conducted an independent investigation on the OPD and disclaims any liability or responsibility relating thereto.

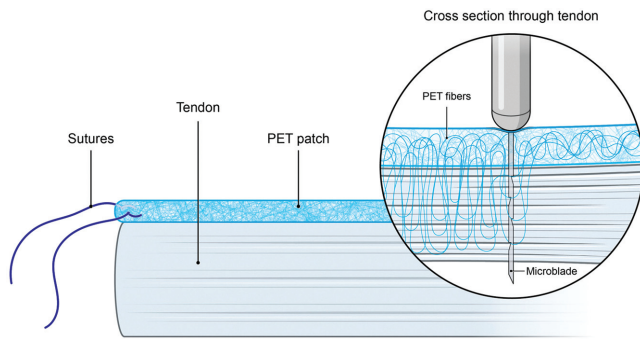


Figure 2. Conceptual diagram depicting direct fiber interlocking of nonwoven patch fibers into the underlying tendon. A suture-free patch-to-tendon configuration was used for the in vivo study of healing. For the in vivo study, a load-bearing suture was attached only to the patch (not passed through the tendon). This suture was then used to affix the tendon to its bony insertion by way of transosseous fixation (in vivo) or to a uniaxial test machine (ex vivo). PET, polyethylene terephthalate.

infraspinatus tendon tear.^{16-19,21,27} Healing performance was based on macroscopic observations and histological analyses at 6 and 13 weeks after implantation. This study was approved by the local ethics committee and federal authorities for animal experiments (permission No. ZH184/19).

A model of partial tenotomy of the infraspinatus muscle was used on 8 white Swiss Alpine sheep (age, 2.5 years; preoperative weight, 61-70 kg). The sheep were positioned in left lateral recumbence. After a lateral approach to the right shoulder was made, the insertion area of the infraspinatus area was visualized. The craniocaudal extent of the tendon was measured, and then the caudal half (50% of measured width) of the tendon was released close to its humeral insertion using a No. 11 blade scalpel. After the tendon incision, 2 bone tunnels (2.0 mm diameter) were drilled from the tendon's caudal footprint region toward the lateral aspect of the greater tuberosity of the humerus. The PET patch was folded in half, and 2 No. 2 FiberWire (Arthrex) sutures were passed through the patch fold. In the next step, the patch was secured to the partially cut tendon using only the fiber interlocking instrument, without the use of transtendon suturing. The patch was interlocked across the entire tendon width of the caudal cut portion of the tendon. On each side, the FiberWire sutures were then shuttled through the appropriate bone drill holes using No. 2/0 Supramide (B. Braun) sutures. Together, they were knotted over a buttress plate (7-hole titanium button plate; DePuy Synthes) at the lateral aspect of the greater tuberosity. The fixation was done so that the cut tendon was brought back under tension in contact with its original insertion footprint.

Four steel wire loops were placed with a simple stitch at the 4 corners of the patch of the infraspinatus tendon as markers to track musculotendinous retraction after surgery. One small screw was drilled into the caudal aspect of the greater tubercle, approximately 5 mm caudodistal

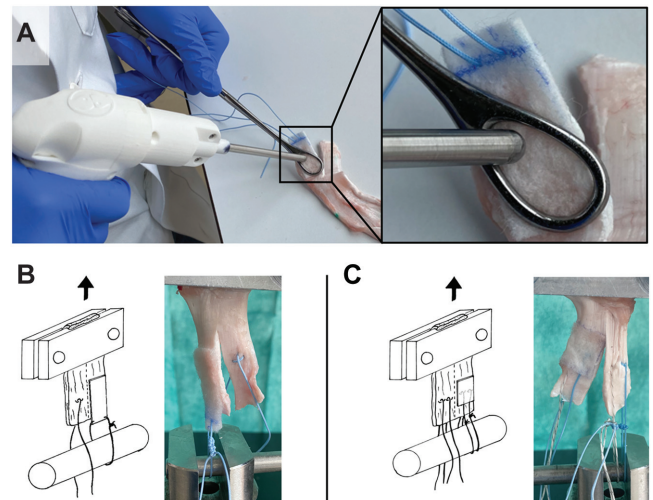


Figure 3. Ex vivo biomechanical testing in pull-to-failure using a uniaxial materials testing machine. (A and B) Interlocking of the nonwoven polyethylene terephthalate (PET) patch onto an ovine infraspinatus tendon using the dedicated surgical instrument to carry microfibers of the patch into the tendon. Tendons were split in half and grasped with either a Mason-Allen suture (control group) or an interlocked PET patch with preattached sutures (intervention group). (C) Augmentation of suture-based repair was investigated by comparing a double row of Mason-Allen sutures (control group) to the same repair but with a PET patch overlaid and interlocked into the underlying tendon.

to the caudal original footprint as a reference point. This allowed the measurement of the following distances: distance between distal steel loops, distance from caudal screw to distal loop, and distance from caudal proximal loop to distal loop. The distance between the individual steel loops and the screws and between the individual steel loops was carefully measured with a caliper.

As a pilot study, 2 sheep were euthanized for analysis at 6 weeks, whereas the remaining 6 sheep were sacrificed 13 weeks after surgery. Immediately after sacrifice, the macroscopic appearance of the implanted patches and the inflammatory status of the surrounding tissues were assessed. Attachment of the implant to the tissue, specifically whether the patch material had de-bonded, was manually probed using forceps. Qualitative evaluations of histological sections were independently performed by 2 experts (S.D., B.v.R.), who focused on tendon-to-bone healing, characterization of host tissue ingrowth into the patch, and aspects of biocompatibility at the patch interfaces to host bone and tendon tissue. The markers placed at the tendon and bone margins were used for quantitative assessment of muscle-tendon retraction over the course of healing and were measured at time of sacrifice using calipers. These displacements were then compared against identical measurements from a recent unrelated study²¹ that was performed using the same animal model but with a standard Mason-Allen (transtendon) suture-based repair. The studies were otherwise identical, being

performed by the same surgeon (B.v.R.) in the same facility, using identical offloading and housing protocols, identical evaluation time points, and identical outcome measures.

Biomechanical Ex Vivo Study

For assessment of the primary mechanical stability of the patch-tendon interface, a total of 16 ovine shoulders from sheep approximately 8 months old were obtained freshly from a local abattoir, dissected, and frozen at -20°C with the infraspinatus tendon-bone footprint and the humerus still intact. After the samples were thawed at room temperature for 6 hours, each infraspinatus tendon was detached at its footprint and longitudinally divided in half to a distance of 3 to 4 cm from the distal end. During thawing and preparation, tendons were prevented from drying by application of phosphate-buffered saline solution. Thickness and width of both tendon halves were measured with a digital caliper, and every tendon was checked for any abnormalities. For purposes of sequential testing, each half (caudal or cranial) was then randomly assigned to 1 of the 2 groups within each experiment to allow pairwise comparison.

A first ex vivo experimental series was performed to assess primary repair strength of the sutureless attachment of the patch to tendon as done in the in vivo experiments (fiber interlocking only, with no sutures passed through the tendon) (Figure 3). Providing a reference for comparison, a control group was established ($n = 8$) that featured a single modified Mason-Allen stitch using a No. 2 FiberWire suture placed approximately 1 cm distal to the tendon end. For the interlocked-patch group ($n = 8$), the PET patch was trimmed to a length of 30 mm and to a width that matched the tendon width (typically 11 mm) before overlaying it to the tendon stump and then interlocking it directly into the tendon using the reciprocating microblade of the instrument (FiberLocker Instrument; ZurIMED Technology). The tendon and patch were secured for fiber interlocking using an oval-shaped Collins tissue-seizing forceps. Attachment of the patch was executed in <1 minute (approximately 35 seconds for an approximately 2-cm^2 patch). The patches were soaked in phosphate-buffered saline for 1 minute before application.

A second ex vivo experimental series was performed to investigate the biomechanical performance of an interlocked patch overlay used to augment an underlying suture-based repair of the tendon. Here, a Mason-Allen suture configuration was used, allowing us to simulate the tendon-grasping sutures used in the previously referenced in vivo study.²¹ This control group ($n = 8$) thus entailed 2 modified Mason-Allen stitches made using No. 2 FiberWire suture material passed through the tendon approximately 1 cm from the distal end (Figure 3B). For the overlay augmentation group ($n = 8$), a PET patch with a length of 20 mm was additionally overlaid atop the 2 modified Mason-Allen stitches (Figure 3C).

All biomechanical testing was performed using a universal materials testing machine mounted with a 10-kN load

cell (Z10; ZwickRoell GmbH). The proximal end of each tendon pair was wrapped in saline-soaked gauze and fixed in a tendon clamp resulting in a 50-mm distal free tendon end and a grip-to-grip separation of 60 mm (Figure 3, B and C). The "bone anchoring" sutures of all respective testing groups were tied with a surgical knot and an additional 5 alternating knots around a horizontal bolt. After one-half of each test pair was pulled to failure (first half of the tendon), the sutures were removed from that side of the tendon, and the sutures of the second side were secured to the lower horizontal bolt and subsequently tested (second half of the tendon). Drawing from Jung et al,²² we preconditioned the tendons with a load of 20 N for 2 minutes to eliminate creep. Cyclic preconditioning was then performed between 10 and 30 N at 1 Hz (force dependent; 0.5 seconds for 20-N force difference) for 10 cycles to stabilize the viscous response. Subsequently, the samples were loaded to failure with an increase in displacement at a constant displacement rate of 1 mm/s.

Statistical Analysis of In Vivo Study Marker Displacement and Biomechanical Ex Vivo Data

Statistical comparisons of marker displacements in the present in vivo study to the data set²¹ using Mason-Allen repair were made using an unpaired Student *t* test. For analysis of ex vivo mechanical data, an a priori power analysis was conducted on the basis of ex vivo biomechanical test results from Wagner et al,⁴⁷ with a sample size of 8 specimens predicted to allow detection of functionally relevant changes in maximal pullout strength. Because controls and intervention samples were sourced from the same infraspinatus tendon, pairwise statistical comparisons could be made to account for biological variation. Normal distribution of the data was confirmed using the Shapiro-Wilk normality test. The paired *t* test was used to compare the biomechanical differences between the control group and the intervention group. In case of nonnormal distribution, the 2 groups were compared using a Wilcoxon matched-pairs signed-rank test. The threshold for statistical significance was set at $P \leq .05$ for all comparisons. All statistical analyses were performed using GraphPad Prism 9.0.0 (GraphPad Software).

RESULTS

In Vivo Study

Macroscopic histological assessment revealed no evidence of adverse tissue reactions or capsule formation and minimal fibrosis at both 6 weeks ($n = 2$) and 13 weeks ($n = 6$). Mechanical probing of the patch using forceps revealed no de-bonded zones between the patch or infraspinatus tendon in any animal at any assessed time point. Macroscopic assessment suggested that the underlying tendon was viable with no detected tissue necrosis in any animal at any time point.

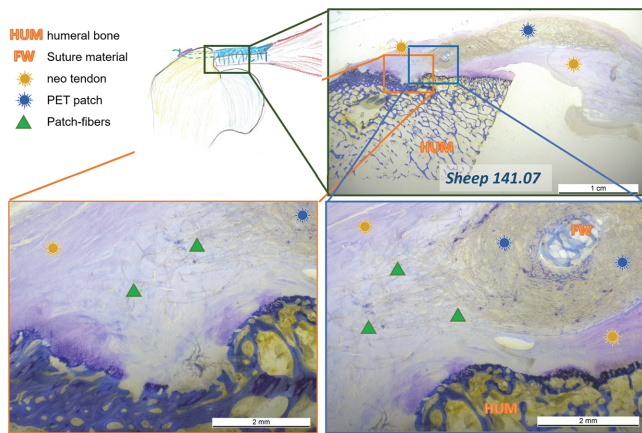


Figure 4. Typical histological findings at 13 weeks. Interaction with surrounding tissue indicated uniform and highly aligned tissue ingrowth. No apparent adverse tissue reactions were detected. Cartilaginous tissue reorganization consistent with a stable insertion to the footprint was generally noted, as well as calcification-like reactions at the distal insertion to the footprint. PET, polyethylene terephthalate.

Microscopic histological examination of poly(methyl methacrylate)-embedded tissue sections by 2 independent and experienced assessors (B.v.R., S.D.) revealed the patch to be histologically well integrated to the tendon tissue at both 6 and 13 weeks, with a characteristically uniform and continuous histological transition between the implant and the tendon. Fibrous tissue ingrowth to the patch was qualitatively aligned to the functional axis of the muscle-tendon unit (Appendix Figure A1, available in the online version of this article).

At the 6-week point (n = 2), the host tissue response was qualitatively determined to be noninflammatory, with foreign body giant cells being sparsely distributed in the tissue in a manner consistent with normal postsurgical physiological healing around implanted nonresorbable materials. Macrophages were rarely observed, whereas singular lymphocytes could occasionally be located in the vicinity of vessels. Plasma cells were rare, whereas a mild periosteal reaction was found at the margins of the bone tunnels. Neovascularization and new tissue formation were noted throughout the patch.

At the 13-week point, fewer immune cells were observed than at 6 weeks, and foreign body giant cells were clearly reduced compared with the tissue sections from the 6-week point. Implants at 13 weeks were determined to be well integrated into the host tissue, featuring longitudinally aligned ingrown tissue structure that was qualitatively more compact than the tissue ingrowth observed at 6 weeks. Overall, 13-week histological results gave the impression of a mature and viable tendon-like tissue structure within the patch with some loose connective tissue around newly formed vessels. At the bony interface, metaplasia to a more chondrogenic tissue including the presence of glycosaminoglycans (qualitatively indicated by the histological stains) (Figure 4) was found mostly close to the insertion site, a reaction that is indicative of normal tendon-to-bone healing. Progenitor cells with a fibroblast-like appearance were visible. At the footprint, some remodeling activity was noted with a tendency for ossification at the insertion site—again, an expected reaction with remodeling after healing. Most of the tendons were well inserted to their footprint, and slight retraction was observed in only 1 sheep where the patch had already slightly protruded over the underlying tendon at the time of surgery. The neovascularization noted at 6 weeks was still evident

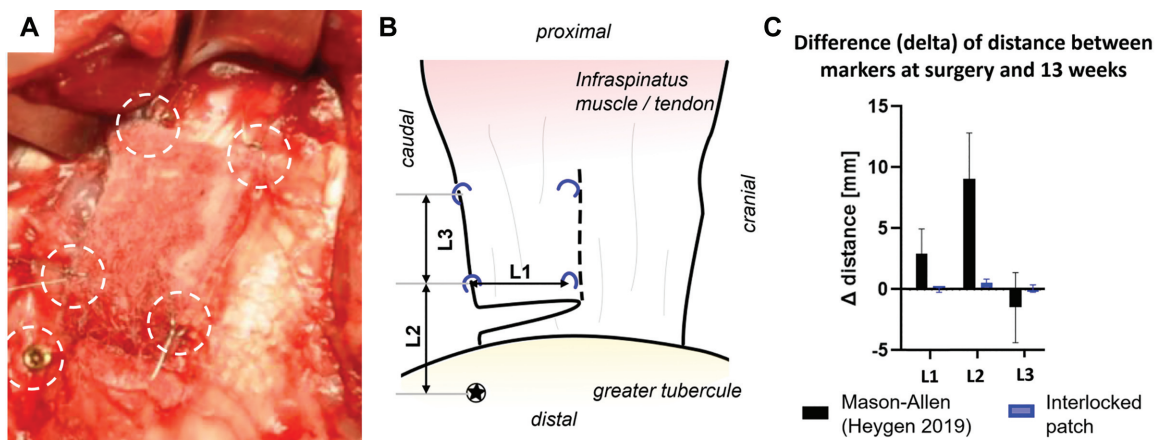


Figure 5. In vivo musculotendinous retraction over 13 weeks of healing. (A) Image of repair site directly after attachment of all markers and a screw (circles). (B) Schematic drawing of measured distances using 4 steel wire loops (semicircles) and a screw (circled star) to track musculotendinous retraction after surgery. (C) Differences of measured distances comparing marker images during surgery and after sacrifice shown in comparison to the Mason-Allen data from a recent study²¹ using an identical model with standard transosseous fixation by 2 rows of Mason-Allen stitches without additional augmentation. L1, caudal-cranial distance between distal steel loops; L2, proximal-distal distance from caudal screw to caudal distal loop; L3, proximal-distal distance from caudal proximal loop to caudal distal loop.

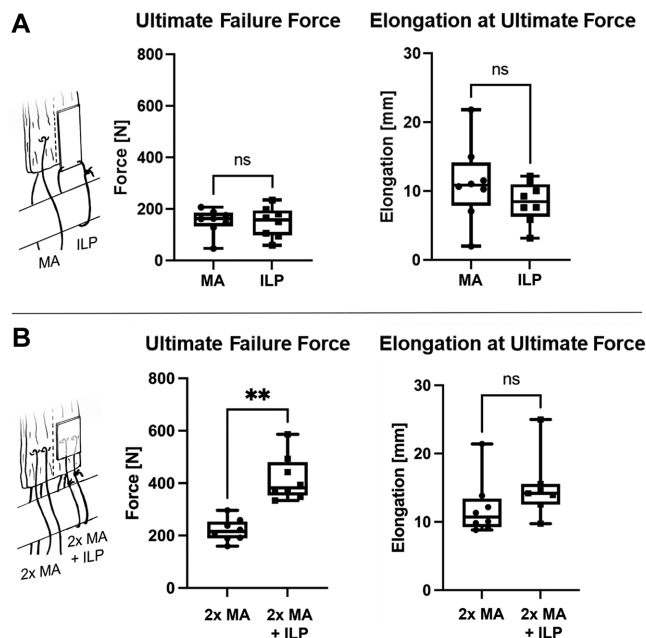


Figure 6. Biomechanical results from sheep cadaveric shoulders, comparing ex vivo suture repair versus interlocked patch augmentation at $t = 0$. (A) Mason-Allen (MA) suture repair versus sutureless interlocked patch (ILP) fixation. (B) Two rows of Mason-Allen suture repair (2x MA) versus an additional interlocked patch that is added on top of the repair (2x MA + ILP). Box plots with median and whiskers from minimum to maximum. ** $p < 0.01$; ns, not significant. t , time.

at 13 weeks. The native tendon otherwise appeared to be viable and well preserved over its entire length, and only minimal musculotendinous retraction was measured after 13 weeks (Figure 5).

Ex Vivo Study

There was no significant difference in repair strength between a single Mason-Allen stitch and sutureless fixation of the interlocked patch (154 ± 49 N vs 150 ± 58 N, respectively; $P = .25$) (Figure 6A). When using the PET patch overlay augmentation to an underlying suture-based repair, load to failure was nearly doubled (from 221 ± 43 N to 417 ± 86 N; $P = .0015$) (Figure 6B). For both configurations used in the ex vivo experiments, there was no difference in repair stiffness under physiological loads or elongation at ultimate force.

DISCUSSION

We describe a novel surgical method for suture-free attachment of a biomaterial patch to tendon. The approach uses a barbed microneedle to interlock fibers of a nonwoven medical felt into the underlying tissue. The method is simple, sutureless, and fast (attachment time < 1 minute),

offering potential to reduce surgical complexity and associated operating time over suture-based patch attachment to medial tissues. Despite the technical simplicity of this approach, ex vivo testing showed mechanical equivalency of suture-free tendon attachment to the purchase afforded by a conventional Mason-Allen stitch. When used as an augmenting overlay to a double-row Mason-Allen stitch, the fiber interlocked overlay increased construct failure strength by nearly 2-fold. In vivo, we could show that interlocking a PET patch to the tendon supported tissue ingrowth at both the tendon and bone interfaces and protected against the severe retraction of the musculotendon unit that characterizes this animal model.²¹

Failure rates of arthroscopically repaired, moderately sized rotator cuff tendon tears remain stubbornly high,^{4,7,38} with failures most often occurring at the suture-tendon interface.¹³ It is generally accepted that patch augmentation offers potential to improve tissue healing and clinical outcomes,¹⁴ and > 20 different types of rotator cuff tendon repair patches have received regulatory approval for surgical use.¹¹ However, patch augmentation remains technically demanding and time intensive if sutures are used for fixation.^{28,29}

Our in vivo testing using an ovine model of acute infraspinatus tendon defect demonstrated robust tissue ingrowth at the interlocked nonwoven PET patch interface with no de-bonding from the underlying tendon. The elicited healing response featured characteristics of healthy cellular ingrowth with appropriately directed tissue formation and negligible fibrosis. Furthermore, minimal musculotendinous retraction was observed in vivo (Figure 5), suggesting that the patch functionally outperformed suture-only attachment.²¹ Our ex vivo testing (Figure 6) suggested that this was most likely achieved by avoiding suture migration (also called “cheese wiring”) through the tendon over the course of healing.

These conclusions we drew are based on data from an animal model. Although the sheep shoulder is the best-established large animal model of rotator cuff repair,^{9,19,20,46} it must be recognized that the ovine infraspinatus differs from that of humans in both its anatomic characteristics and its healing potential. In some respects, it is both a worst-case model of a noncompliant patient with uncontrolled postoperative loads and a best-case model of tissue healing. In any case, the results we report with respect to retraction of the musculotendinous unit represent a fair demonstration that patch augmentation via interlocking offers potential to mitigate suture cut-through, a primary culprit in clinical failure in humans.

Other limitations should be considered. Tendon biomechanical and biological characteristics are complex, and anatomic and physiological differences between human and sheep rotator cuff tendons demand caution in interpreting the potential clinical relevance of the present study.⁵ Moreover, all experiments were performed via open surgery, which does not reflect the visual and anatomic constraints that confront a surgeon during an arthroscopic procedure. Finally, the in vivo data on musculotendinous unit retraction (Figure 5) rely on a comparison with an independently performed previous study rather

than use of a dedicated control group.²¹ We believe that this limitation is acceptable because both studies were recently performed by the same veterinary surgeon in the same expert facility, using a well-established sheep model of uniform breed and age, with identical pre- and postsurgical protocols, and with all experimental data being evaluated anew by the same assessor, who was blinded to the experimental group, and using identical endpoints. In this sense, we consider the present study to represent a blocked-study design with little likelihood that potential biases from the study design could explain the highlighted differences. Despite the limitations of the study, we consider our data to collectively support the conclusion that mechanical fiber interlocking represents a feasible and potentially promising new approach to patch-augmented rotator cuff repair.

With regard to the nonwoven patch material we used, medical felts have a long history of clinical use and have been successfully used to augment tendon repair in pre-clinical animal models^{24,30} and human applications.^{37,39} In 1986, Ozaki et al³⁰ described the use of felt patches to cover irreparable tears of the rotator cuff. Kimura et al²⁴ reconstructed the infraspinatus tendon defects of 31 beagle shoulders using polytetrafluoroethylene felt grafts. Healing of the tendon was attained in 30 of the 31 cases. Kimura et al reported a 5-fold increase of tensile strength of the tendons over the course of healing, with reported failure strength of 61 N immediately after implantation and 306 N after 12 weeks of healing. The canine study used ultrasound to reveal a robust fibrous tissue ingrowth among the patch felt fibers. Similar findings have been reported in the literature using a felt graft in a rat shoulder model.³⁰ Finally, the literature also contains a report of successful interpositional bridging of large rotator cuff tears in humans using a nonwoven patch to treat “irreparable rotator cuff tear” in a small case series of 5 patients, with positive subjective and objective outcomes reported after a 10-year follow-up.³⁹ The results of our own in vivo study on sheep (Figure 5) thus seem to echo the reported success of this small clinical series.

CONCLUSION

Testing in an ovine model of rotator cuff tendon repair suggested that surgical interlocking of a nonwoven PET medical felt can provide effective biomechanical performance, support functional tissue ingrowth, and help avoid musculotendinous retraction after surgical tendon repair.

A Video Supplement for this article is available online.

REFERENCES

1. Barber FA, Herbert MA, Boothby MH. Ultimate tensile failure loads of a human dermal allograft rotator cuff augmentation. *Arthroscopy*. 2008;24(1):20-24.

2. Batty LM, Norsworthy CJ, Lash NJ, et al. Synthetic devices for reconstructive surgery of the cruciate ligaments: a systematic review. *Arthroscopy*. 2015;31(5):957-968.
3. Boszotta H, Helperstorfer W. Long-term results of arthroscopic implantation of a Trevira prosthesis for replacement of the anterior cruciate ligament. Article in German. *Aktuelle Traumatologie*. 1994;24(3):91-94.
4. Buess E, Steuber KU, Waibl B. Open versus arthroscopic rotator cuff repair: a comparative view of 96 cases. *Arthroscopy*. 2005;21(5):597-604.
5. Burgio V, Civera M, Rodriguez Reinoso M, et al. Mechanical properties of animal tendons: a review and comparative study for the identification of the most suitable human tendon surrogates. *Processes*. 2022;10(3):485.
6. Cai YZ, Zhang C, Jin RL, et al. Arthroscopic rotator cuff repair with graft augmentation of 3-dimensional biological collagen for moderate to large tears: a randomized controlled study. *Am J Sports Med*. 2018;46(6):1424-1431.
7. Chalmers PN, Tashjian RZ. Patch augmentation in rotator cuff repair. *Curr Rev Musculoskelet Med*. 2020;13(5):561-571.
8. Ciampi P, Scotti C, Nonis A, et al. The benefit of synthetic versus biological patch augmentation in the repair of posterosuperior massive rotator cuff tears: a 3-year follow-up study. *Am J Sports Med*. 2014;42(5):1169-1175.
9. Coleman SH, Fealy S, Ehteshami JR, et al. Chronic rotator cuff injury and repair model in sheep. *J Bone Joint Surg Am*. 2003;85(12):2391-2402.
10. Consigliere P, Bernasconi A, Dimock R, Narvani AA. Clinical outcomes and structural integrity rate of arthroscopic augmented rotator cuff repairs using extracellular porcine matrix patch. *Shoulder Elbow*. 2022;14(1)(suppl):38-51.
11. Cook JA, Baldwin M, Cooper C, et al. Findings from the patch augmented rotator cuff surgery (PARCS) feasibility study. *Pilot Feasibility Stud*. 2021;7(1):163.
12. Cowling P, Hackney R, Dube B, et al. The use of a synthetic shoulder patch for large and massive rotator cuff tears—a feasibility study. *BMC Musculoskelet Disord*. 2020;21(1):213.
13. Cummins CA, Murrell GA. Mode of failure for rotator cuff repair with suture anchors identified at revision surgery. *J Shoulder Elbow Surg*. 2003;12(2):128-133.
14. de Andrade ALL, Garcia TA, Brandao HS, et al. Benefits of patch augmentation on rotator cuff repair: a systematic review and meta-analysis. *Orthop J Sports Med*. 2022;10(3):23259671211071146.
15. Ferguson DP, Lewington MR, Smith TD, Wong IH. Graft utilization in the augmentation of large-to-massive rotator cuff repairs: a systematic review. *Am J Sports Med*. 2016;44(11):2984-2992.
16. Fluck M, Kasper S, Benn MC, et al. Transplant of autologous mesenchymal stem cells halts fatty atrophy of detached rotator cuff muscle after tendon repair: molecular, microscopic, and macroscopic results from an ovine model. *Am J Sports Med*. 2021;49(14):3970-3980.
17. Gerber C, Meyer DC, Fluck M, et al. Muscle degeneration associated with rotator cuff tendon release and/or denervation in sheep. *Am J Sports Med*. 2017;45(3):651-658.
18. Gerber C, Meyer DC, Frey E, et al. Neer Award 2007: reversion of structural muscle changes caused by chronic rotator cuff tears using continuous musculotendinous traction. An experimental study in sheep. *J Shoulder Elbow Surg*. 2009;18(2):163-171.
19. Gerber C, Meyer DC, Schneeberger AG, Hoppeler H, von Rechenberg B. Effect of tendon release and delayed repair on the structure of the muscles of the rotator cuff: an experimental study in sheep. *J Bone Joint Surg Am*. 2004;86(9):1973-1982.
20. Gerber C, Schneeberger AG, Perren SM, Nyffeler RW. Experimental rotator cuff repair: a preliminary study. *J Bone Joint Surg Am*. 1999;81(9):1281-1290.
21. Heygen M. *Evaluating the Efficacy of DYNACORD™ Suture*. Dissertation. University of Zurich; 2019. Accessed August 18, 2023. <https://doi.org/10.5167/uzh-176815>
22. Jung C, Spreiter G, Audigé L, Ferguson SJ, Flury M. Patch-augmented rotator cuff repair: influence of the patch fixation technique on primary biomechanical stability. *Arch Orthop Trauma Surg*. 2016;136(5):609-616.

23. Karuppaiah K, Sinha J. Scaffolds in the management of massive rotator cuff tears: current concepts and literature review. *EFORT Open Rev.* 2019;4(9):557-566.
24. Kimura A, Aoki M, Fukushima S, Ishii S, Yamakoshi K. Reconstruction of a defect of the rotator cuff with polytetrafluoroethylene felt graft: recovery of tensile strength and histocompatibility in an animal model. *J Bone Joint Surg Br.* 2003;85(2):282-287.
25. Lapner P, Henry P, Athwal GS, et al. Treatment of rotator cuff tears: a systematic review and meta-analysis. *J Shoulder Elbow Surg.* 2022;31(3):e120-e129.
26. Li L, Bokshan SL, Ready LV, Owens BD. The primary cost drivers of arthroscopic rotator cuff repair surgery: a cost-minimization analysis of 40,618 cases. *J Shoulder Elbow Surg.* 2019;28(10):1977-1982.
27. Meyer DC, Gerber C, Von Rechenberg B, Wirth SH, Farshad M. Amplitude and strength of muscle contraction are reduced in experimental tears of the rotator cuff. *Am J Sports Med.* 2011;39(7):1456-1461.
28. Morris JH, Malik AT, Hatef S, et al. Cost of arthroscopic rotator cuff repairs is primarily driven by procedure-level factors: a single-institution analysis of an ambulatory surgery center. *Arthroscopy.* 2021;37(4):1075-1083.
29. Narvani AA, Imam MA, Polyzois I, et al. The “pull-over” technique for all arthroscopic rotator cuff repair with extracellular matrix augmentation. *Arthrosc Tech.* 2017;6(3):e679-e687.
30. Ozaki J, Fujimoto S, Masuhara K, Tamai S, Yoshimoto S. Reconstruction of chronic massive rotator cuff tears with synthetic materials. *Clin Orthop Relat Res.* 1986;202:173-183.
31. Parchi PD, Ciapini G, Paglialunga C, et al. Anterior cruciate ligament reconstruction with LARS artificial ligament—clinical results after a long-term follow-up. *Joints.* 2018;6(2):75-79.
32. Patel S, Caldwell JM, Doty SB, et al. Integrating soft and hard tissues via interface tissue engineering. *J Orthop Res.* 2018;36(4):1069-1077.
33. Porter M, Shadbolt B, Ye X, Stuart R. Ankle lateral ligament augmentation versus the modified Broström-Gould procedure: a 5-year randomized controlled trial. *Am J Sports Med.* 2019;47(3):659-666.
34. Santoni BG, McGilvray KC, Lyons AS, et al. Biomechanical analysis of an ovine rotator cuff repair via porous patch augmentation in a chronic rupture model. *Am J Sports Med.* 2010;38(4):679-686.
35. Schlegel TF, Abrams JS, Bushnell BD, Brock JL, Ho CP. Radiologic and clinical evaluation of a bioabsorbable collagen implant to treat partial-thickness tears: a prospective multicenter study. *J Shoulder Elbow Surg.* 2018;27(2):242-251.
36. Seitz H, Marlovits S, Schwendenwein I, Müller E, Vécsei V. Biocompatibility of polyethylene terephthalate (Trevira® Hochfest) augmentation device in repair of the anterior cruciate ligament. *Biomaterials.* 1998;19(1):189-196.
37. Seker V, Hackett L, Lam PH, Murrell GAC. Evaluating the outcomes of rotator cuff repairs with polytetrafluoroethylene patches for massive and irreparable rotator cuff tears with a minimum 2-year follow-up. *Am J Sports Med.* 2018;46(13):3155-3164.
38. Severud EL, Ruotolo C, Abbott DD, Nottage WM. All-arthroscopic versus mini-open rotator cuff repair: a long-term retrospective outcome comparison. *Arthroscopy.* 2003;19(3):234-238.
39. Shepherd HM, Lam PH, Murrell GA. Synthetic patch rotator cuff repair: a 10-year follow-up. *Shoulder Elbow.* 2014;6(1):35-39.
40. Smith C, Ajuied A, Wong F, et al. The use of the ligament augmentation and reconstruction system (LARS) for posterior cruciate reconstruction. *Arthroscopy.* 2014;30(1):111-120.
41. Smolen D, Haffner N, Mittermayr R, et al. Application of a new polyester patch in arthroscopic massive rotator cuff repair—a prospective cohort study. *J Shoulder Elbow Surg.* 2020;29(1):e11-e21.
42. Tanaka N, Sakahashi H, Hirose K, Ishima T, Ishii S. Augmented subscapularis muscle transposition for rotator cuff repair during shoulder arthroplasty in patients with rheumatoid arthritis. *J Shoulder Elbow Surg.* 2006;15(1):2-6.
43. Tauro TM, Wagner KR, DeFroda SF, et al. Technical note: arthroscopic rotator cuff repair with patch augmentation with acellular dermal allograft. *Arthrosc Tech.* 2022;11(2):e121-e125.
44. Thon S, Savoie FH III. Rotator cuff repair: patch the shoulder. *Arthroscopy.* 2019;35(4):1014-1015.
45. Tischer T, Lenz R, Breinlinger-O'Reilly J, Lutter C. Cost analysis in shoulder surgery: a systematic review. *Orthop J Sports Med.* 2020;8(5):2325967120917121.
46. Turner AS. Experiences with sheep as an animal model for shoulder surgery: strengths and shortcomings. *J Shoulder Elbow Surg.* 2007;16(5)(suppl):S158-S163.
47. Wagner E, Wagner P, Ortiz C, et al. Biomechanical cadaveric evaluation of partial acute peroneal tendon tears. *Foot Ankle Int.* 2018;39(6):741-745.